Supporting Information

Tripodal exTTF-CTV hosts for fullerenes

Elisa Huerta,[†] Helena Isla,[‡] Emilio M. Pérez,[‡,§] Carles Bo,[†] Nazario Martín*[,‡,§] and Javier de Mendoza,*[,†]

Institute of Chemical Research of Catalonia (ICIQ), Av. Països Catalans, 16, 43007 Tarragona, Spain, Departamento de Química Orgánica, Facultad de Química, Universidad Complutense, 28040 Madrid, and IMDEA-nanociencia, 28049 Madrid, Spain

Materials and Experimental Methods:

All chemicals were purchased from commercial sources and used without further purification. Solvents were dried and distilled using conventional methods[1] or using a Solvent Purification System (SPS).NMR spectra were performed on Bruker Avance 400 (^{1}H: 400 MHz, ^{13}C: 100 MHz) or Bruker Avance 500 (^{1}H: 500 MHz, ^{13}C: 125 MHz) Ultrashield spectrometers. Deuterated solvents used are indicated in each case. Chemical shifts (δ) are expressed in ppm, and are referred to the residual peak of the solvent. High performance liquid chromatography (HPLC) analyses were carried out on an Agilent Technologies Serie 1100 apparatus using a reverse phased C_{18} Sunfire column (4.6x150mm, 5µm) from Waters, with UV-diode array and mass detectors. The mobile phase used was acetonitrile 100% at 25 °C. HPLC grade solvents were purchased from Scharlab and Carlo Erba and were used with no further purification**.** Mass analysis was performed in Waters LCT Premier (ESI or APCI mode), and Bruker MALDI-TOF spectrometers. UV titrations were done in a Shimadzu UV-2401PC UV-Vis spectrophotometer with a thermostated (7–60 ºC) sample holder (optical range from 190 to 1100 nm). Thin layer chromatography (TLC) was performed on Alugram Sil G-25/UV254-coated aluminium sheets (Macherey-Nagel) with detection by UV at 254 nm. Electrochemistry was carried out in a PARSTAT 2273 potentiostat from Princeton Applied Research with 2 A as maximum current and 1fA of resolution. HPLC or high purity solvents were used to prepare the solutions, which were bubbled with argon 5 minutes before each measurement. To avoid sample concentration, the argon flow was passed through a reservoir flask containing the solvent mixture which was placed before the working cell. Working electrode was glassy carbon; counter electrode was Pt wire and reference electrode was Ag/AgCl. Working electrode was polished between each measurement with 3µm silica. Pt wire was also cleaned between each measurement with a mixture of sulphuric acid and hydrogen peroxide, then water and methanol, and dried in an oven. The CW-EPR spectra were obtained at room temperature on a Bruker EMX 10/12 spectrometer at X band (9.84 GHz) with the ER4123D dielectric resonator, using a 4.0 mm outer-

[1] Perrin, D. D.; Amarego, W. L. F.; Perrin, D. R. Purification of Laboratory Chemicals, 2nd ed., Pergamon Press, Oxford, **1980**

diameter quartz tube (Norell, Landisville, NJ, USA) for liquid solutions. Solutions were freeze-thaw deareated prior to measurements. The UV irradiation in situ EPR measurements was carried out with a high pressure mercury lamp (Bruker, UV Irradiation System, ER 202 UV). The distance between the lamp and the sample was 60 cm. Instrumental settings were as follows: center field = 3365 G; sweep width = 1000 G; microwave power = 12.6 mW: modulation amplitude = 1,00 G; modulation frequency = 100 kHz; receiver gain = 10^5; time constant = 163.84 ms; sweep time = 41.94 s; resolution in x = 1024 points; number of scans = 1.

Synthesis of exTTF-CTV:

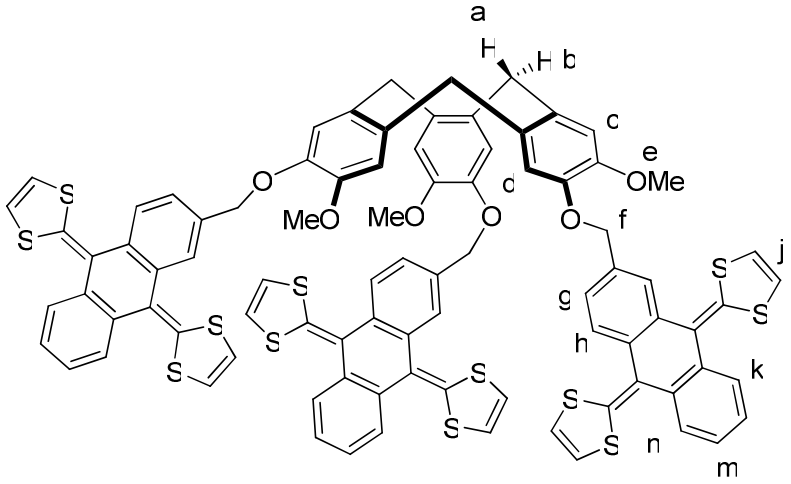

CTV triphenol[2] (25 mg, 0.061 mmol), exTTF methylene alcohol[3] (88 mg, 0.214 mmol) and PPh_3 (57 mg, 0.214 mmol) were mixed together, solved in dry DCM into a round bottom flask and stirred at 0ºC. DIAD (44 µl, 0.214 mmol) was then added and the mixture was allowed to room temperature and stirred 4 days. Solvent was taken up and the residue was purified by flash chromatography in $CHCl_3$/MeOH (1%). **exTTF-CTV** was isolated as a yellow solid in a 46% yield (45 mg). ^{1}H NMR (500 MHz, chlorobenzene-d_5, 353 K) δ (ppm): 8.09 (bs, 3H, H_i); 7.97 (s, 6H, H_k + H_n); 7.93 (d, *J = 8.2 Hz*, 3H, H_h); 7.53 (bd, *J = 8.2 Hz,* 3H, H_g); 7.44 (hidden under solvent signal – see HH COSY, 6H, .H_l + H_m); 7.31 (s, 3H, H_c); 7.12 (s, 3H, H_d); 6.06 (m, 12H, H_j); 5.36 (m, 6H, H_f); 4.92 (d, J =14.0 Hz, 3H, H_a); 3.84 (s, 9H, H_e); 3.73 (d, J = 14.0 Hz, 3H, H_b). HPLC-MS analysis: Sunfire C18, MeCN, 1 mL/min, λ=254 nm, 95% purity. APCI(+) MS: m/z 1584.1 $[M]^+$ (100%).; ESI(+) MS: m/z 1548.2 $[M]^+$ (10%), 792.7 $[M]^{2+}$ (100%). Maldi-TOF MS: 1584.2 $[M]^+$ (100%).

[2] Vériot, G.; Dutasta, J. P.; Matouzenko, G.; Collet, A. *Tetrahedron* **1995**, *51*, 389.

[3] Marshallsay, G. J.; Bryce, M. R. *J. Org. Chem.* **1994**, *59*, 6847.

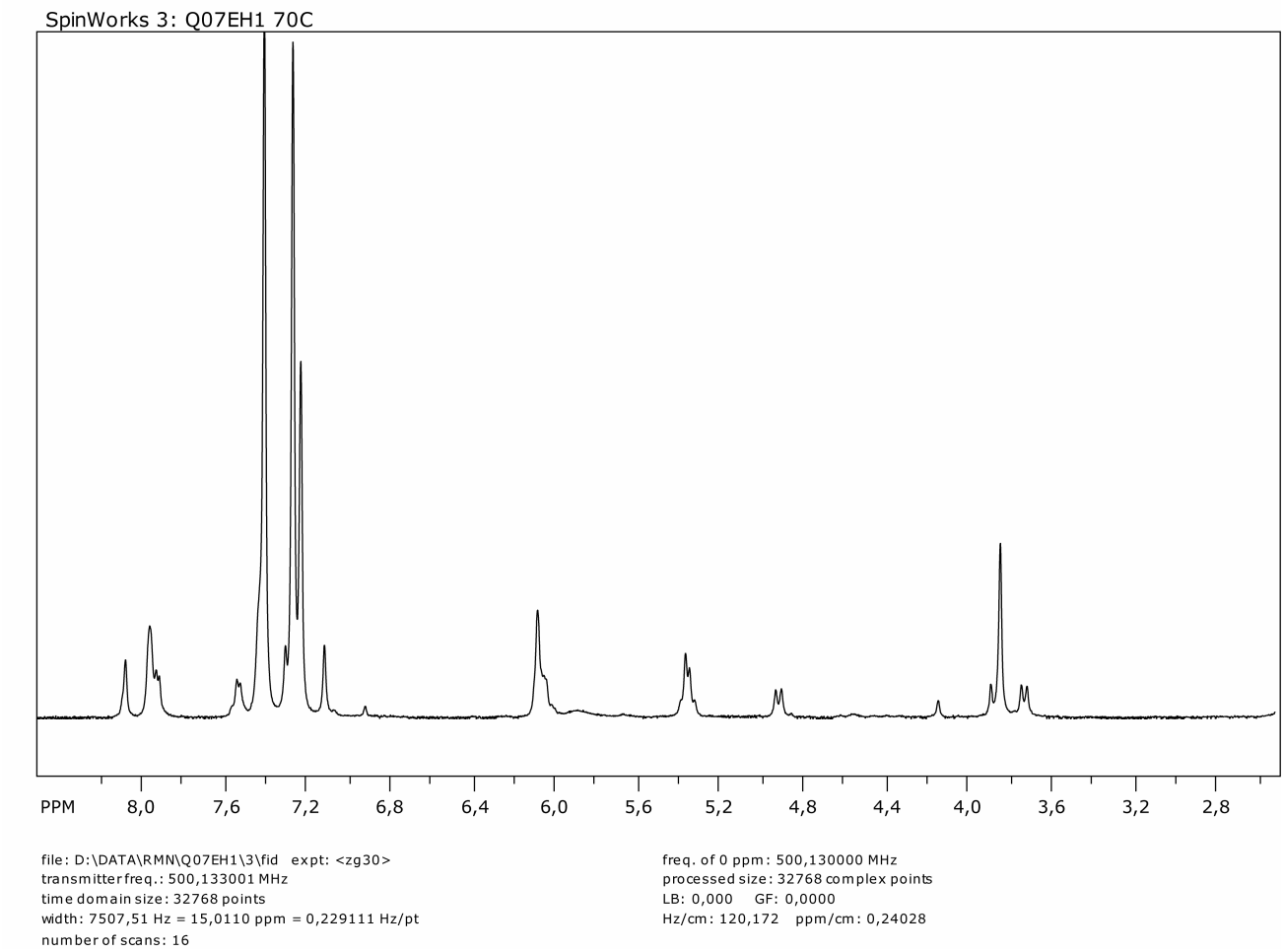

Figure S 1: ^{1}H NMR (chlorobenzene-d_5, 500 MHz, 353 K) of **exTTF-CTV**.

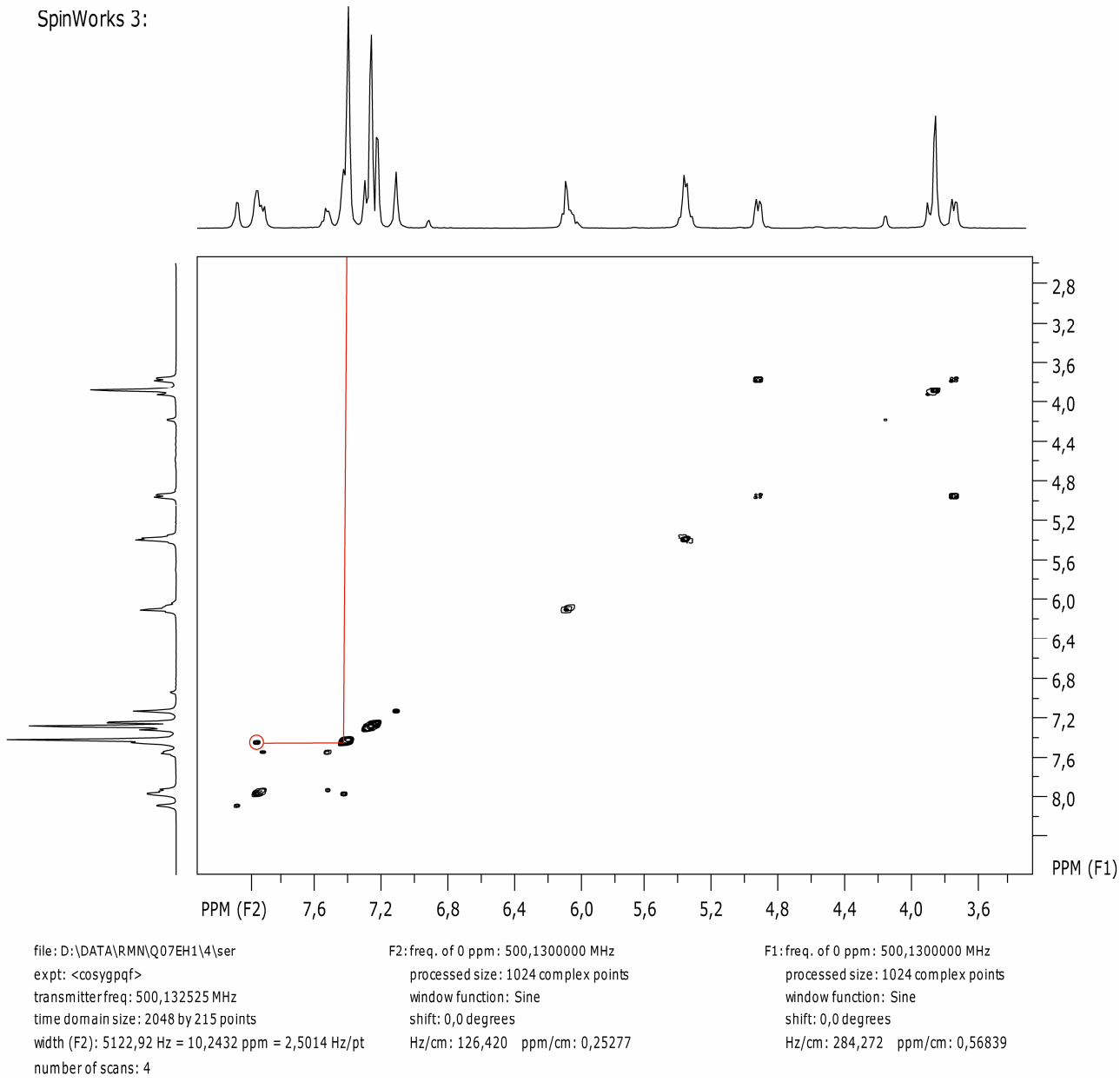

Figure S 2: HH COSY (chlorobenzene-d_5, 500 MHz, 353 K) of **exTTF-CTV.**

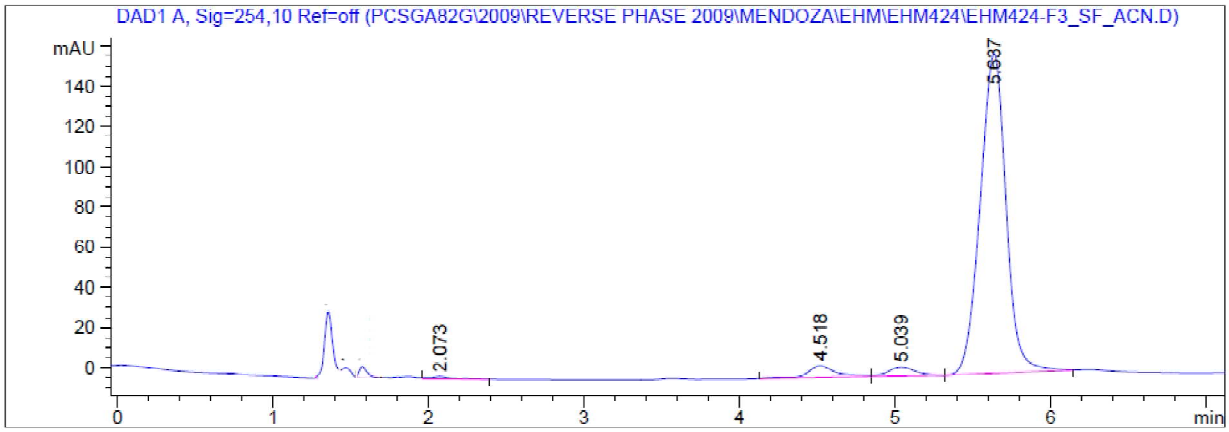

Figure S 3: HPLC profile of **exTTF-CTV**. Sufire C18, acetonitrile, 1 ml/min, λ=254 nm.

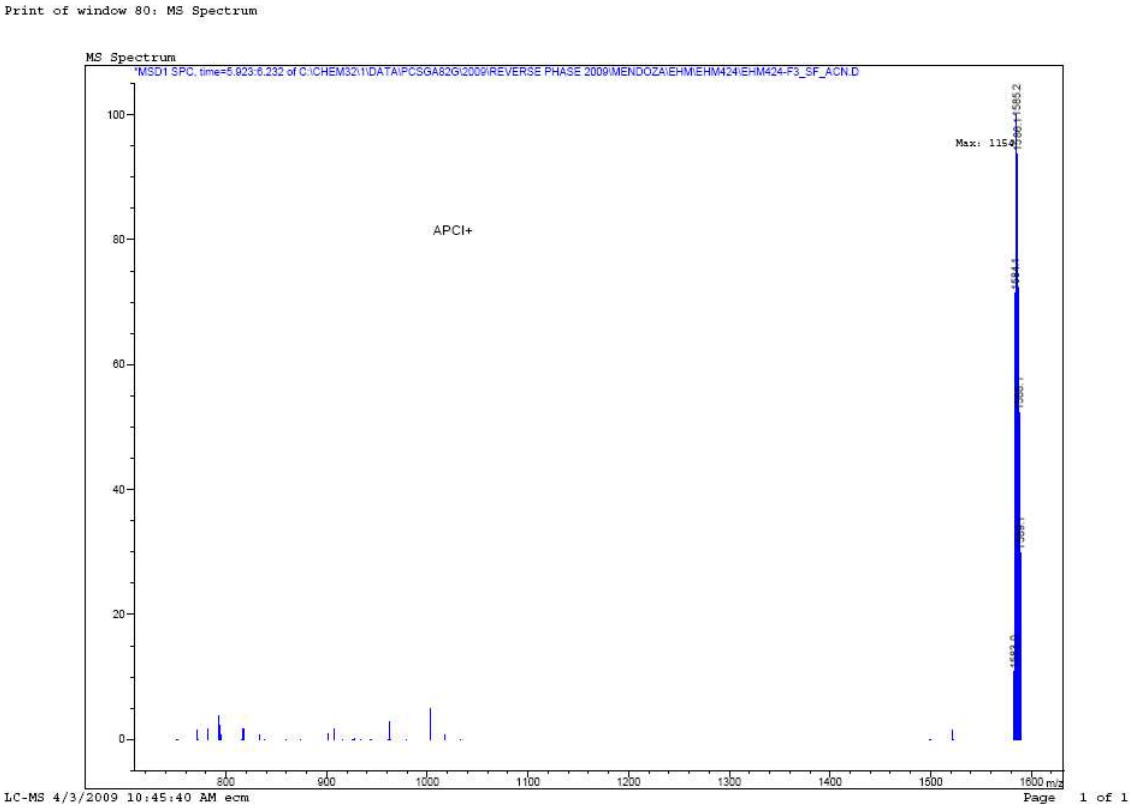

Figure S 4: Atmospheric Pressure Chemical Ionization (APCI+) positive mode of peak at retention time 5.637 min.

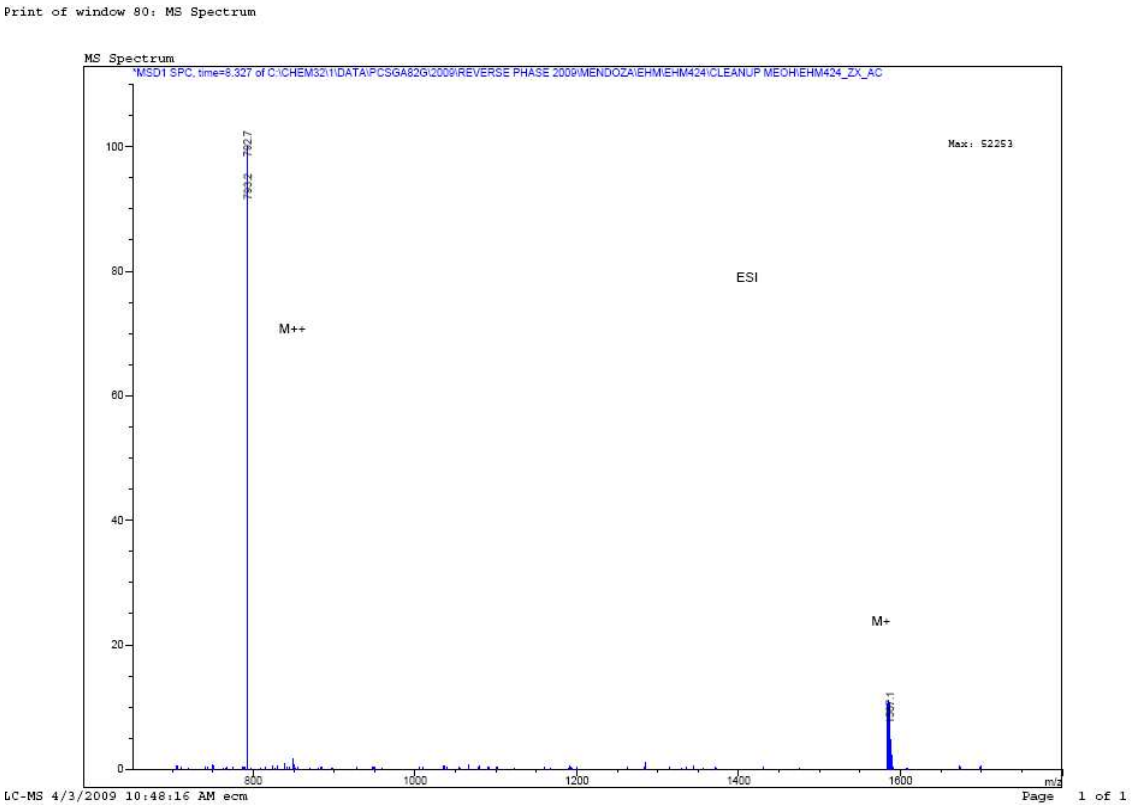

Figure S 5: Electrospray (ESI+) positive mode of peak at retention time 5.637 min.

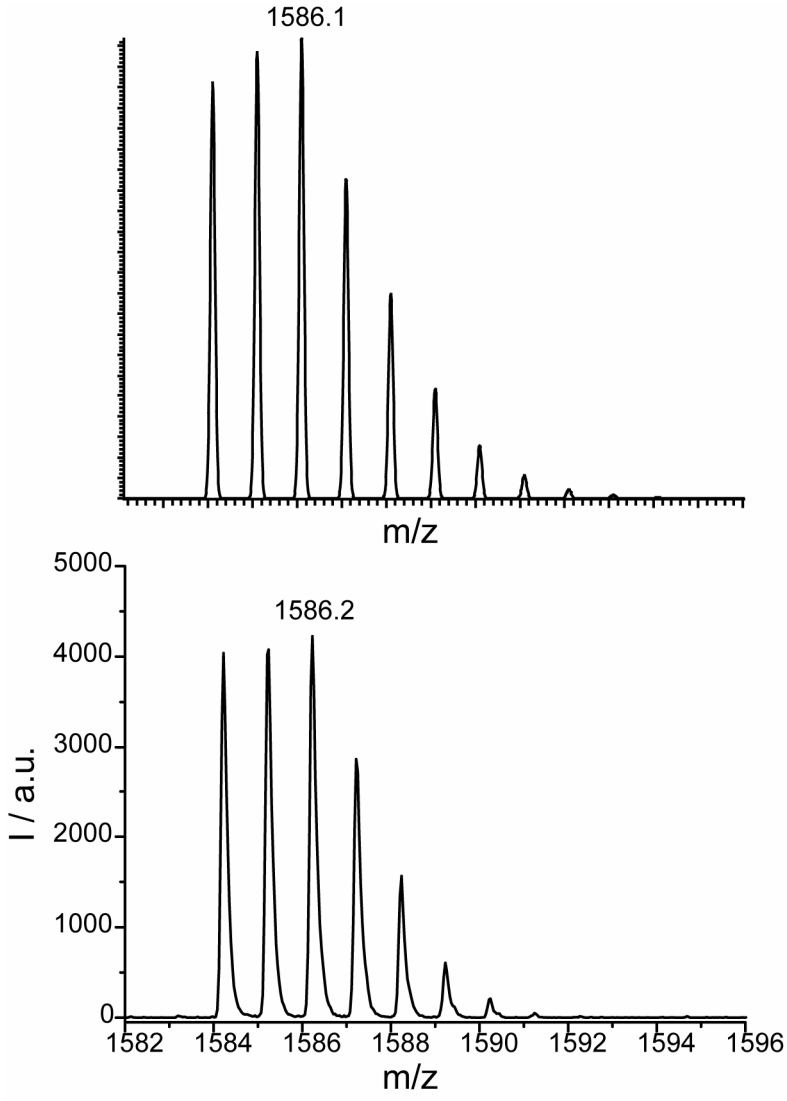

Figure S 6: Isotopic pattern simulated (top) and found (MALDI-TOF+) of **exTTF-CTV**.

Complexation in solution was studied by UV-vis spectroscopy. The stoichiometry of the complexes was studied using the method of Continuous Variations. Experiments were carried out using chlorobenzene as solvent being the concentration of exTTF-CTV**, C_{60} and C_{70} 0.3 mM respectively. In**

Figure S 7 and

Figure S 8 are showed the corresponding Job's Plots.

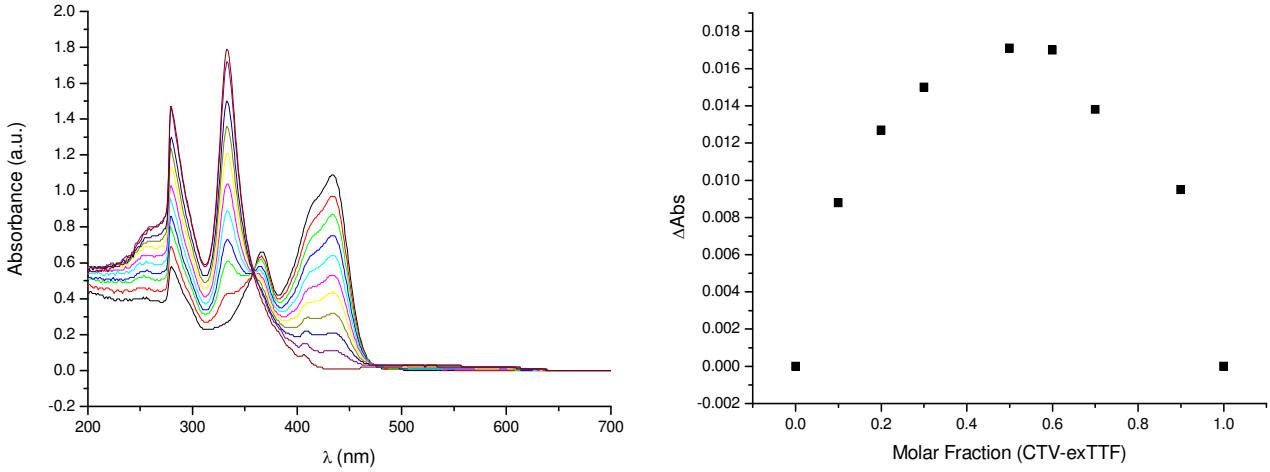

Figure S 7: Job's Plot for complex C_{60}**@exTTF-CTV**. [**exTTF-CTV**] = [C_{60}] = 0.3 mM in chlorobenzene (λ = 436 nm).

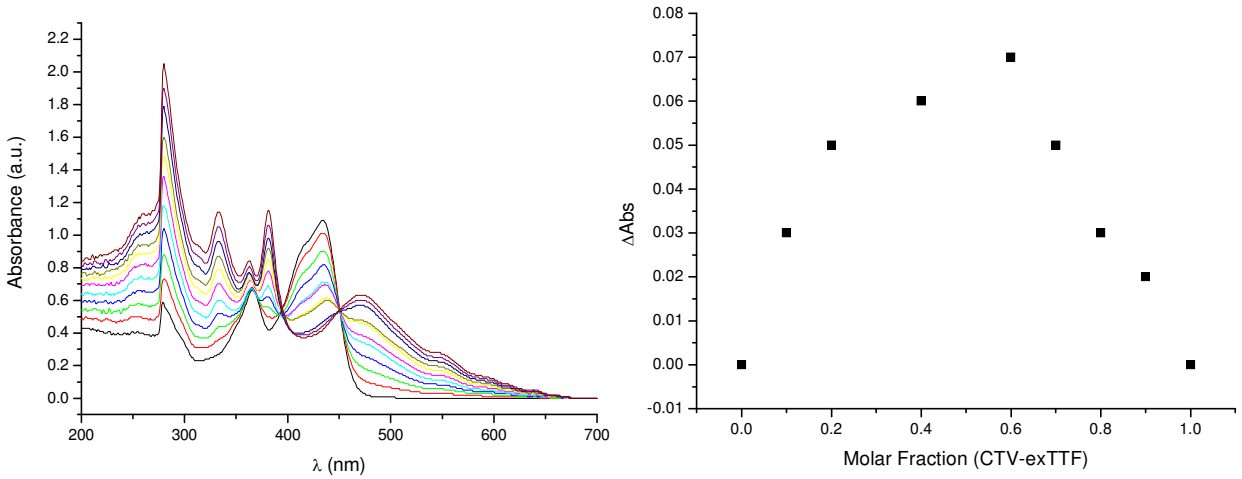

Figure S 8: Job's Plot for complex C_{70}**@exTTF-CTV**. [**exTTF-CTV**] = [C_{70}] = 0.3 mM in chlorobenzene (λ = 436 nm).

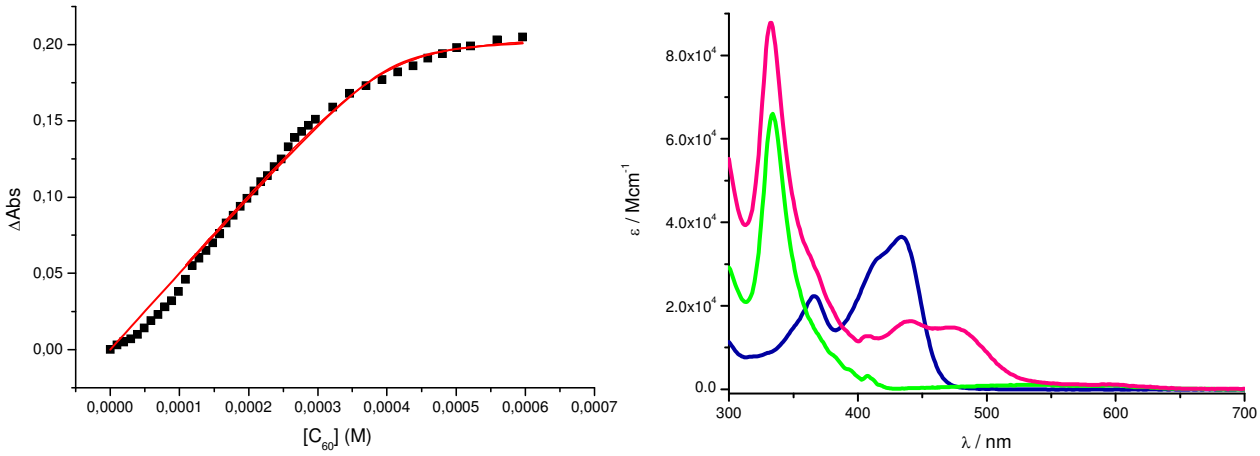

Figure S 9: Binding isotherm (left) and calculated ε (right, pink) for the C_{60}@**exTTF-CTV**.

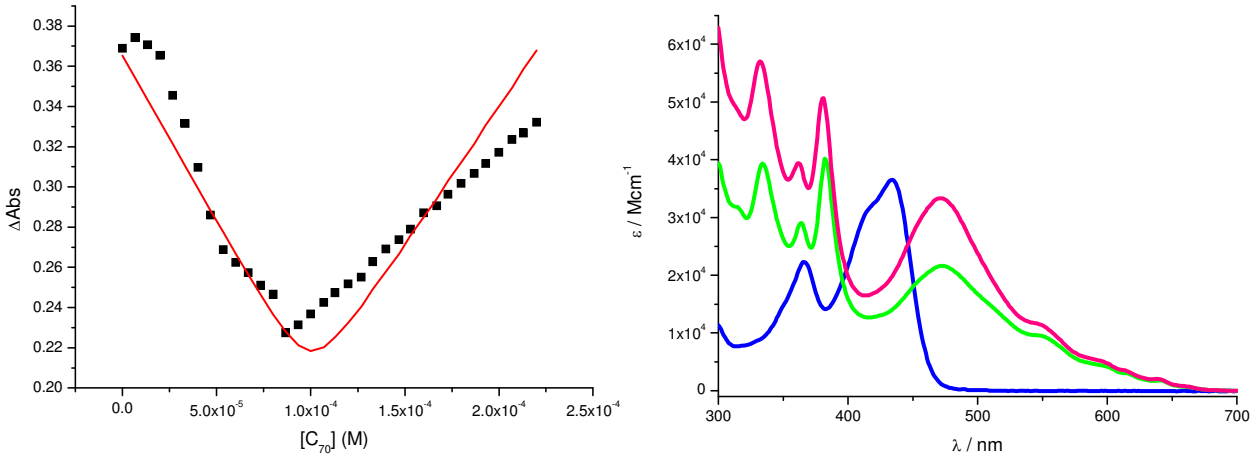

Figure S 10: Binding isotherm (left) and calculated ε (right, pink) for the C_{70}@**exTTF-CTV**.

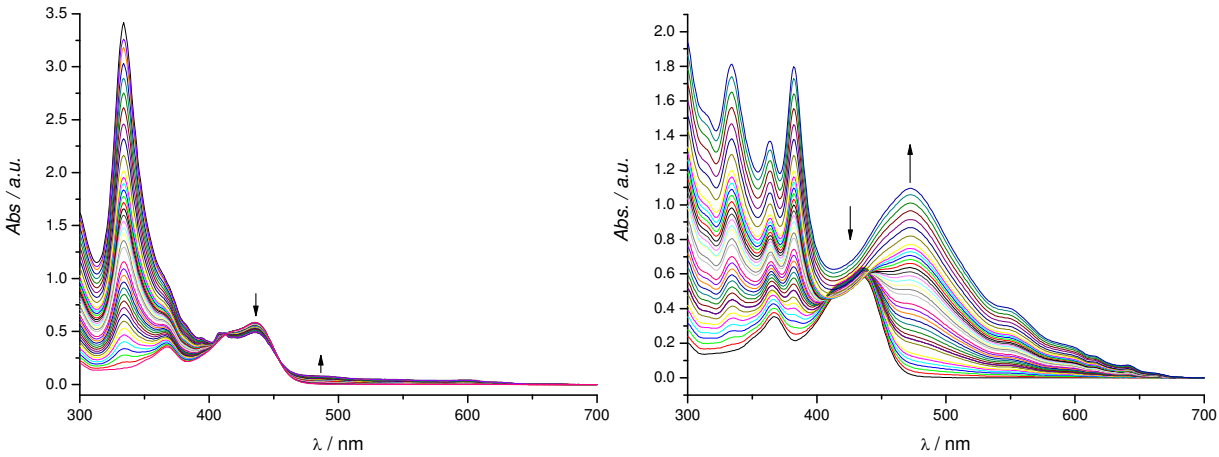

Figure S 11: UV-vis titration of 10^{-5} M solutions of **exTTF-CTV** by additions of 0.1 equivalets of C_{60} (left) and C_{70} (right).

exTTF-CTV and its C_{60} complex were both extensively studied by ^{1}H-NMR. Initially, samples were dissolved in a $CDCl_3/CS_2$ mixture in a 5:2 ratio. At room temperature (Figure S 12, 298 K) the **exTTF-CTV** spectrum shows very broad signals. When the sample was cooled down until 218 K, the spectrum became sharper and a significant splitting and movement of the signals was observed. The effect experimented for a 1:1 mixture of C_{60} and **exTTF-CTV** was quite similar (Figure S 13).

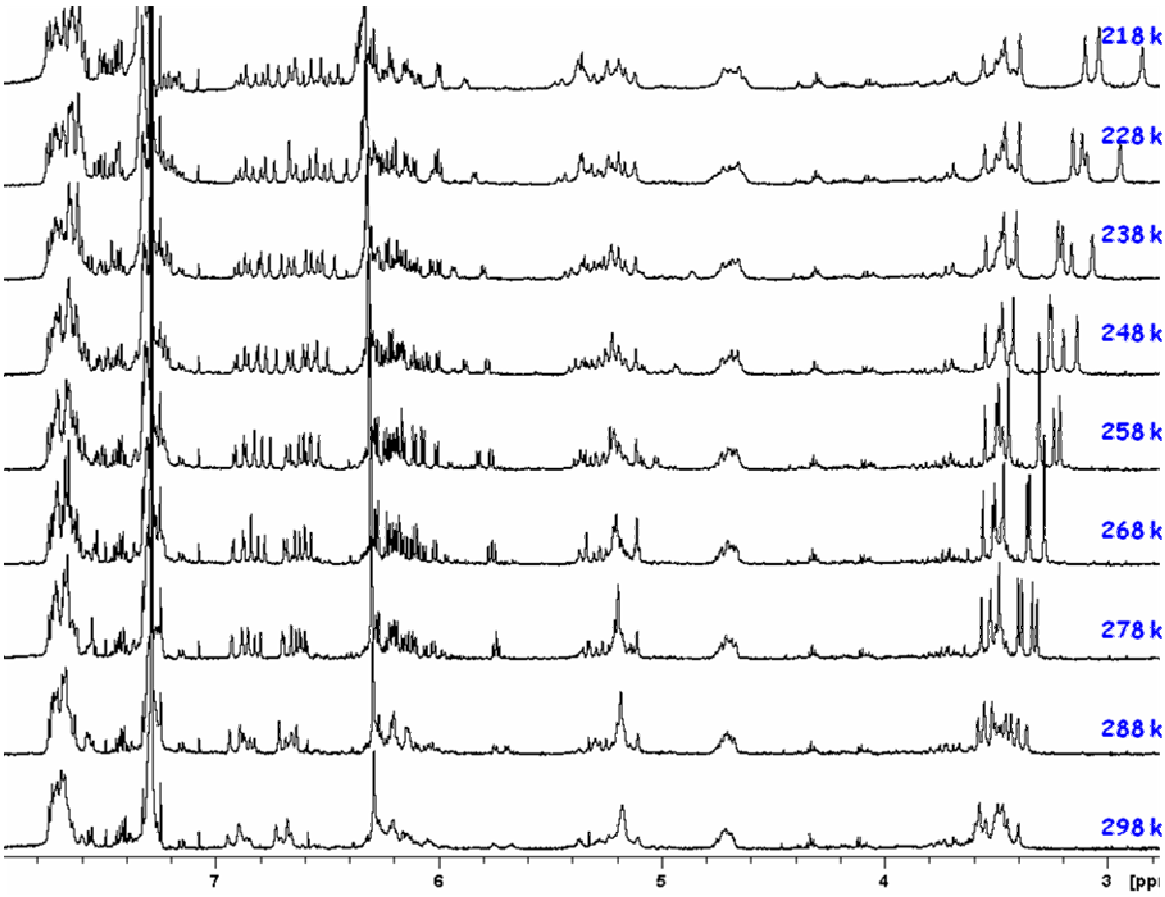

Figure S 12: Variable temperature ^{1}H-NMR experiment (from 25º to -55ºC) of **exTTF-CTV** in $CS_2/CDCl_3$ (5:2) (500 MHz).

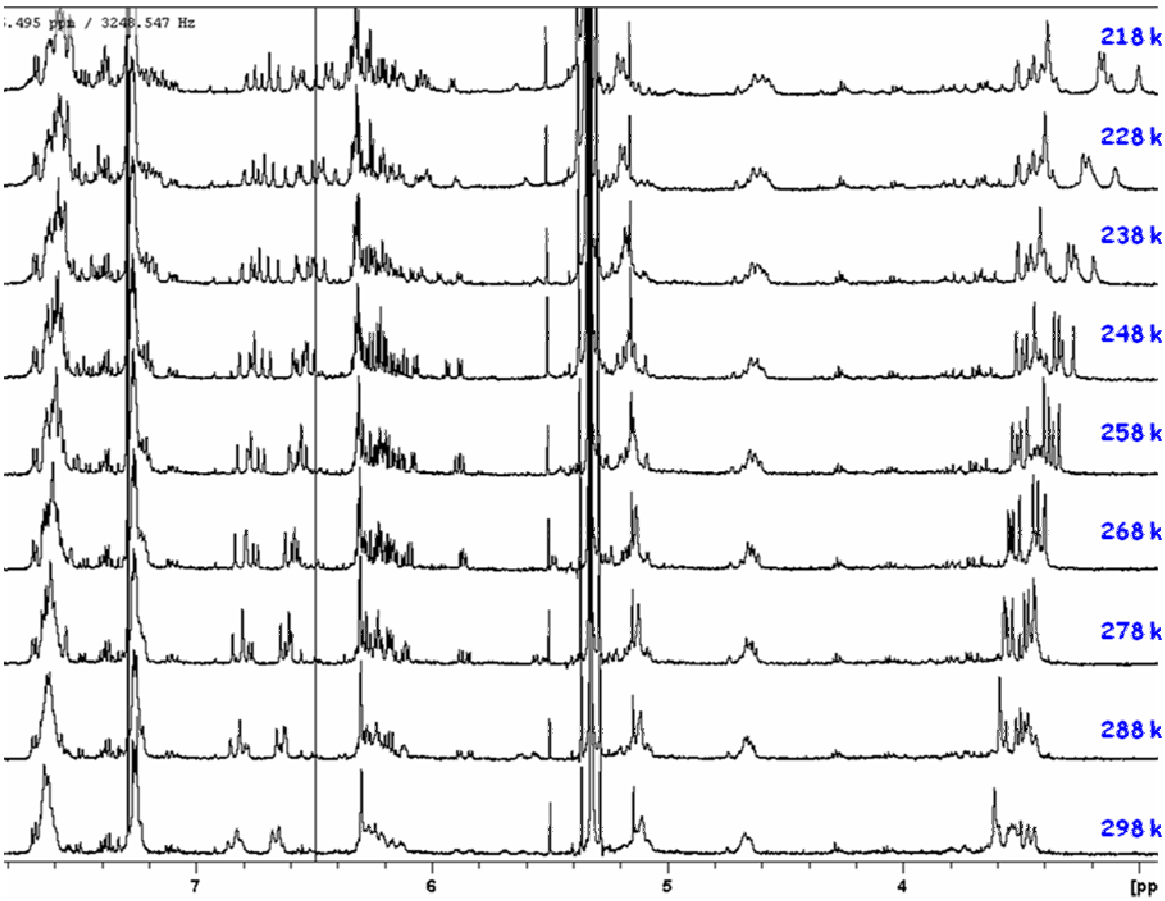

Figure S 13: Variable temperature ^{1}H-NMR experiment (from 25º to -55ºC) of C_{60}@**exTTF-CTV** in $CS_2/CDCl_3$ (5:2) (500 MHz).

In order to carry out high temperature experiment, toluene was used as solvent. Samples were heated up from room temperature to 105 ºC. In the case of **exTTF-CTV** receptor (Figure S 14), some signals were still splited (as the CH_2 who links the CTV and the exTTF at ~ 5 ppm or the OMe group at ~ 3.5 ppm), but in general, the spectrum became simplified and some signals were resolved, as the methylene bridges of CTV scaffold. The same sample was then cooled down (Figure S 15) up to -75 ºC. In this solvent, differently than were chloroform carbon disulphide mixture was used, the signal became broader and no splitting was observed. When C_{60} was added to the receptor (1:1 mixture) no significant changes were observed, maybe because the spectrum was too complicate to distinguish any anisotropic effect due to complexation over receptor signals (Figure S 16 and Figure S 17).

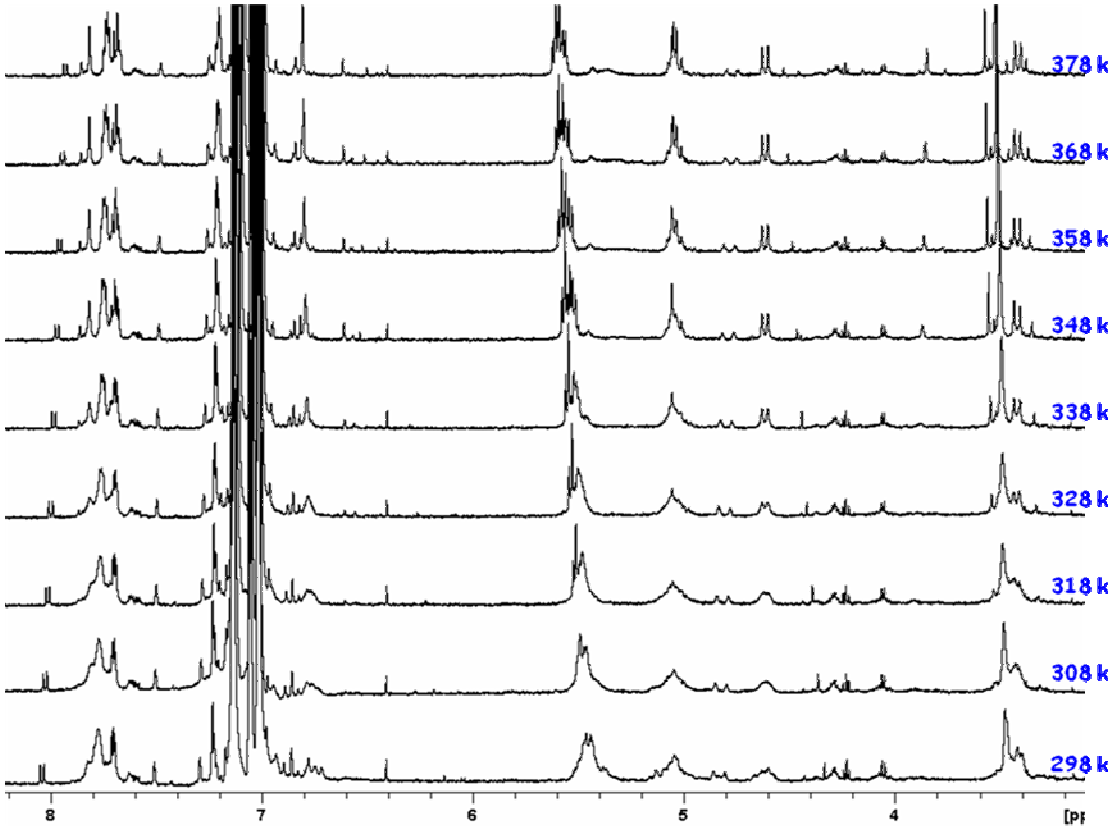

Figure S 14: Variable temperature ^{1}H-NMR experiment (from 25º to 105ºC) of **exTTF-CTV** in toluene (500 MHz).

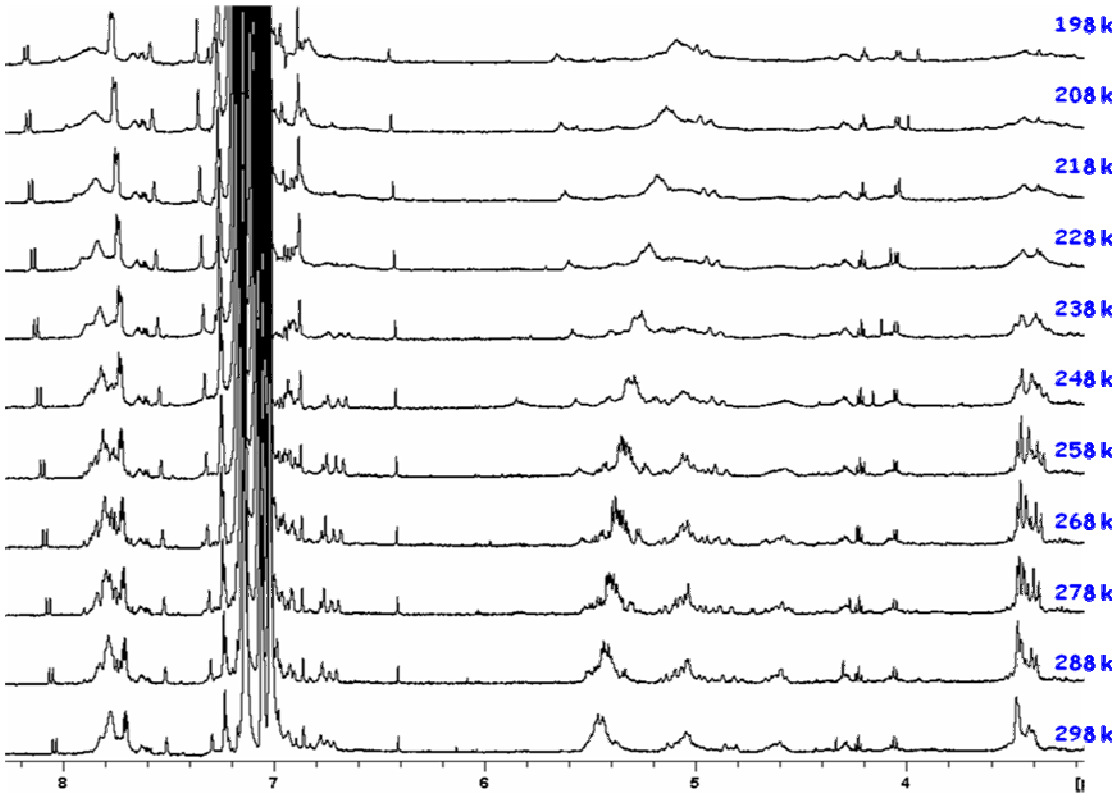

Figure S 15: Variable temperature ^{1}H-NMR experiment (from 25º to -75ºC) of compound **exTTF-CTV** in toluene (500 MHz).

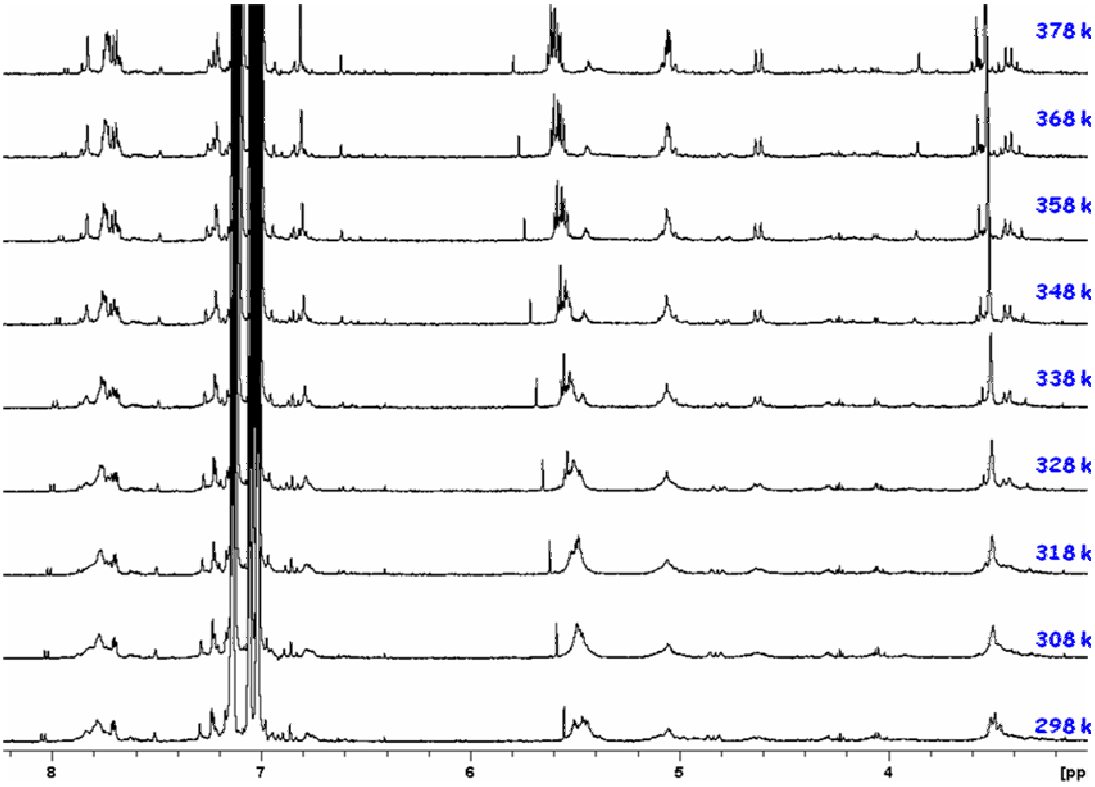

Figure S 16: Variable temperature ^{1}H-NMR experiment (from 25º to 105ºC) of compound **C_{60}@exTTF-CTV** in toluene (500 MHz).

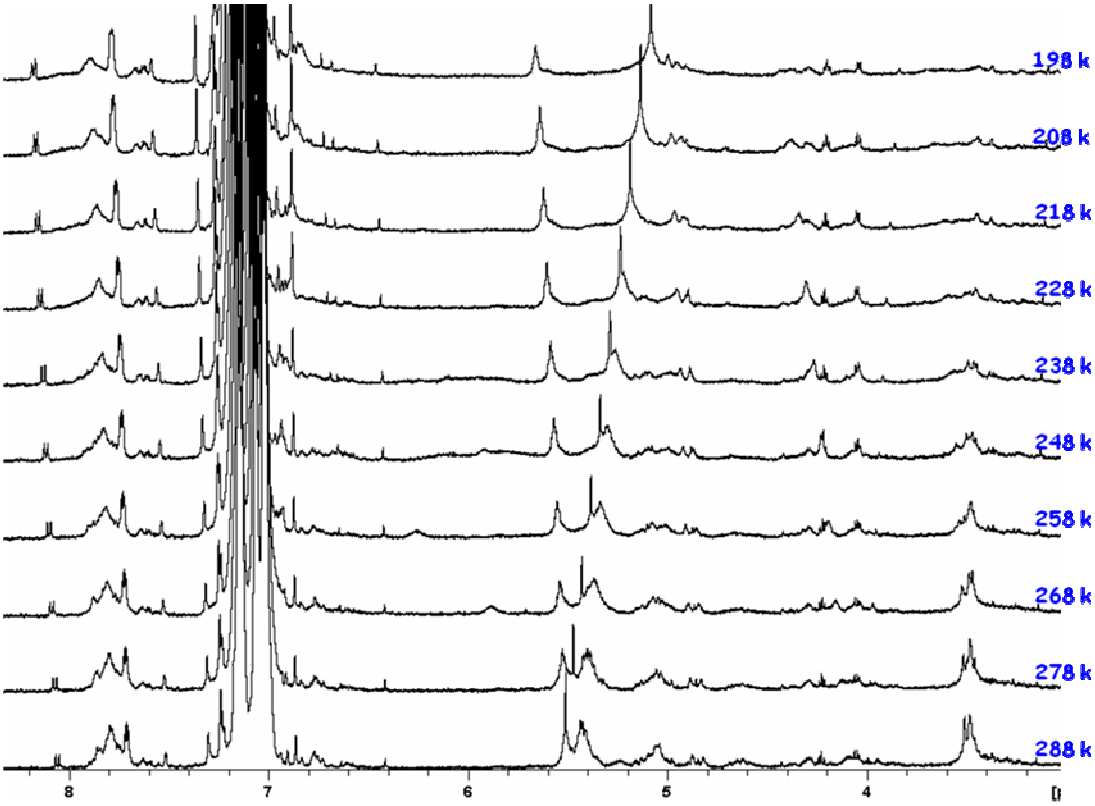

Figure S 17: Variable temperature ^{1}H-NMR experiment (from 25º to -75ºC) of compound C_{60}**@exTTF-CTV** in toluene (500 MHz).

Using chlorobenzene as solvent, the spectrum of **exTTF-CTV** is somehow broadened but resolved and a small shifting of the signals can be observed upon complexation of C_{60}.

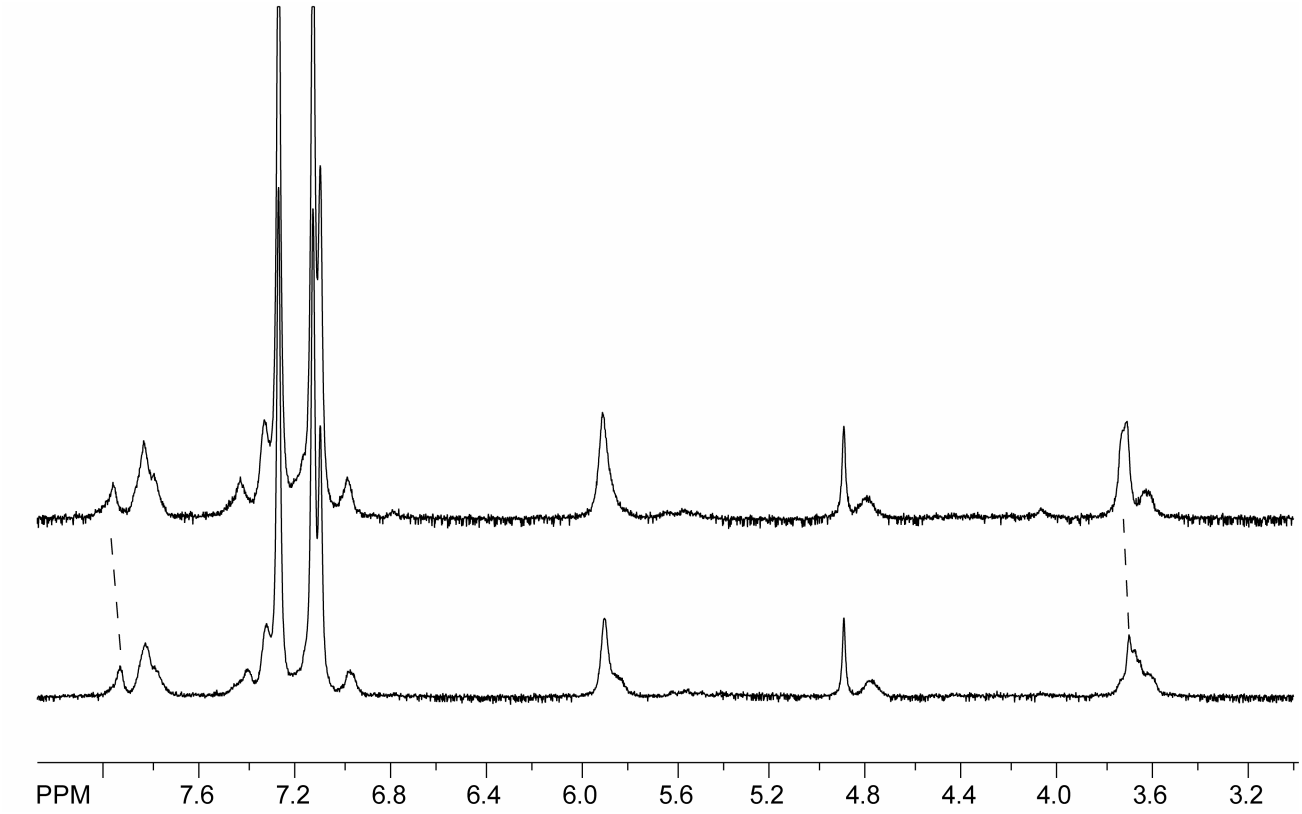

Figure S 18: 1H NMR (d_5-chlorobenzene, 500 MHz, 25ºC) of C_{60}@**exTTF-CTV** (top) and **exTTF-CTV** (bottom).

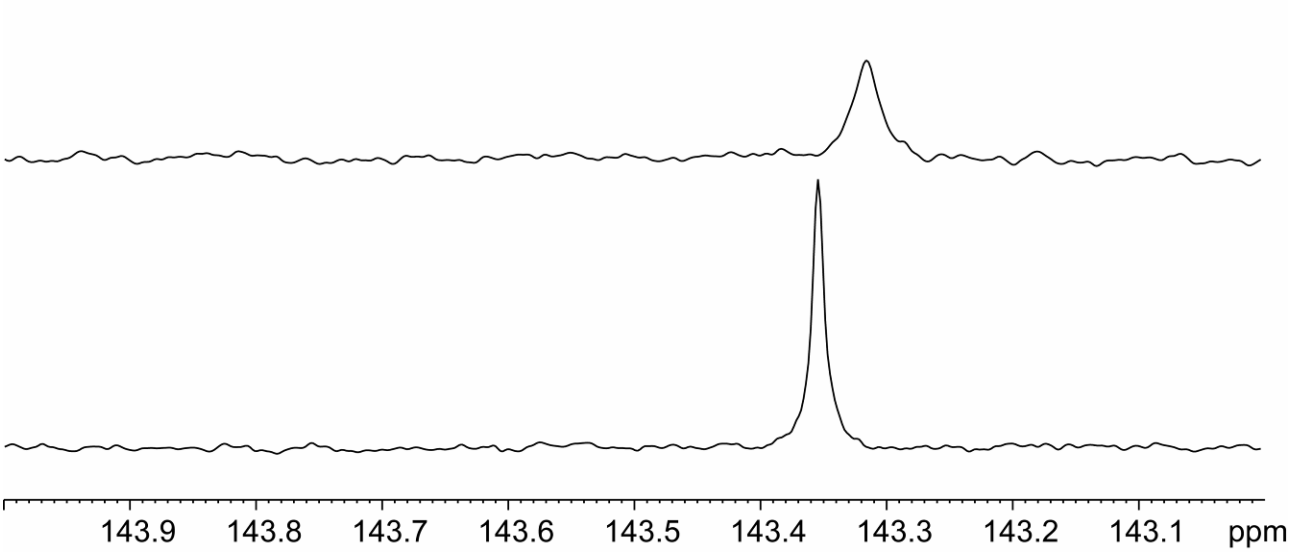

Figure S 19: ^{13}C NMR (d_5-chlorobenzene, 125 MHz, 25ºC) of C_{60}@**exTTF-CTV** (top) and C_{60} (bottom).

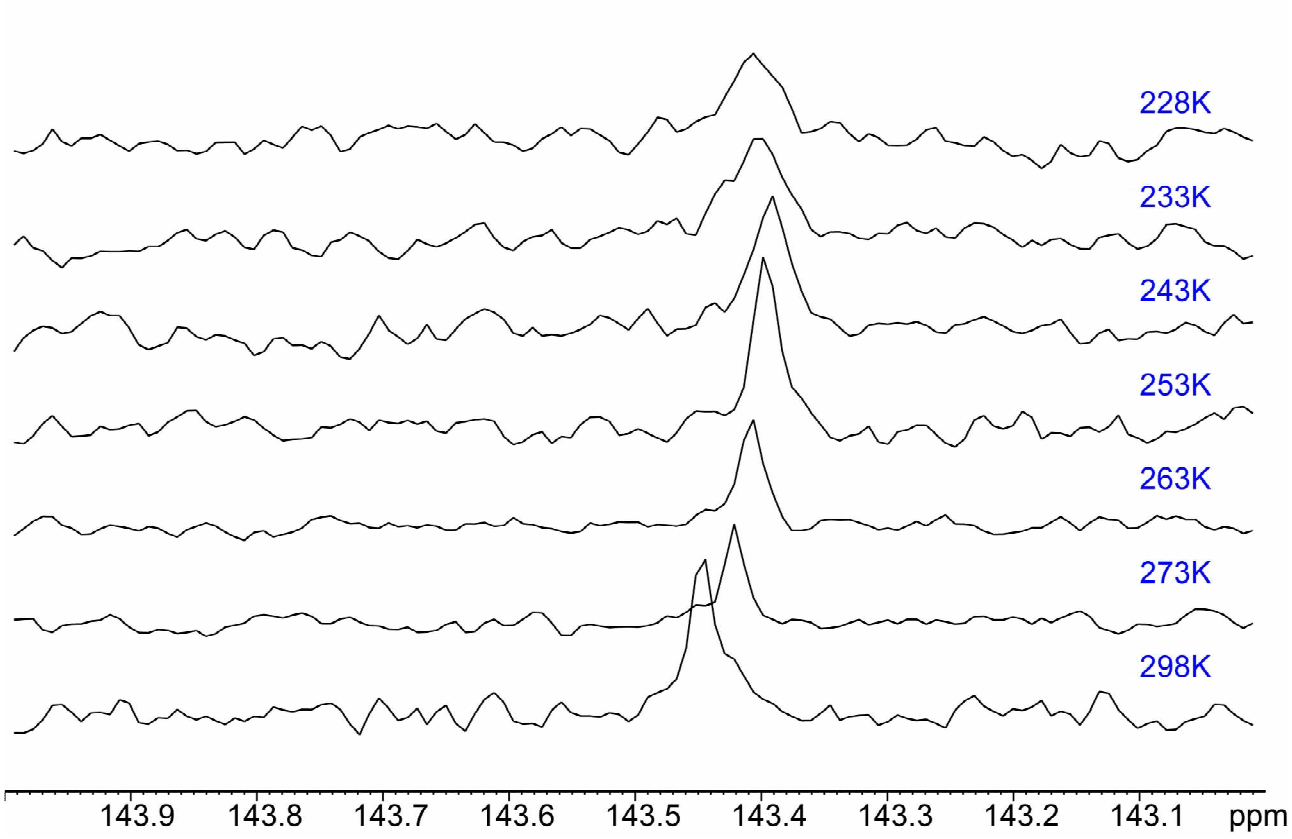

Figure S 20: VT-^{13}C NMR (d_5-chlorobenzene, 75 MHz, from 25 to -45ºC) of C_{60}@**exTTF-CTV**.

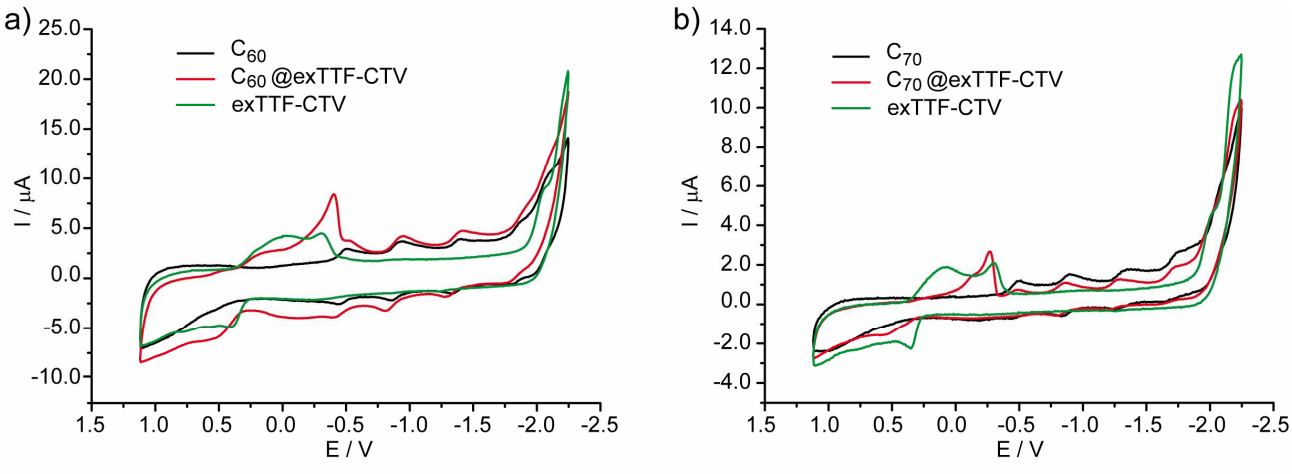

Figure S 21: Cyclic voltammetry measurements of solutions 10^{-5} M of free fullerenes and their complexes in chlorobenzene with 0.1 M of Bu_4NClO_4 as electrolyte. Working electrode: glassy carbon; Counter electrode: Pt wire; Reference electrode Ag/AgCl; Scan rate: 50 mV/s.

DFT Calculations

A theoretical study of the complexes was carried out using a density functional theory (DFT) approach. Calculations to show the electrostatic potential distribution of the fullerenes C_{60} and C_{70} and **exTTF-CTV** receptor were obtained from minimized structures. The electrostatic potential mapped onto an electronic charge density isosurface of the molecules is shown so that, from most negative values to most positive values, the range of colours is red, orange, yellow, green, light blue, dark blue, where green regions are the most neutral ones.

Figure S 22 shows the mapping of the electrostatic potential for C_{60} (left) and C_{70} (right) fullerenes. In the representation, the whole surface is mostly positive, especially in the centre of the pentagonal and hexagonal rings.

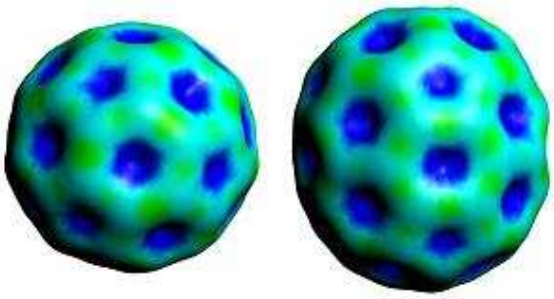

Figure S 22: Mapping of the electrostatic potential onto an electron density isosurface of C_{60} and C_{70} (BP86/DZP).

In case of **exTTF-CTV** (Figure S 23), the entire molecule is mostly negative (red) and the most negative regions are found in the aromatic surfaces of cyclotriveratrylene moiety as well as in the anthracene-like part in exTTF moiety (see inner and side views in Figure S 23). This means that there is not only a perfect match between the concave shape of the receptor and the convex surface of the fullerene, but also an electronic match as the more negative electrostatic potential inside the cavity attracts the positive electrostatic potential of the fullerene.

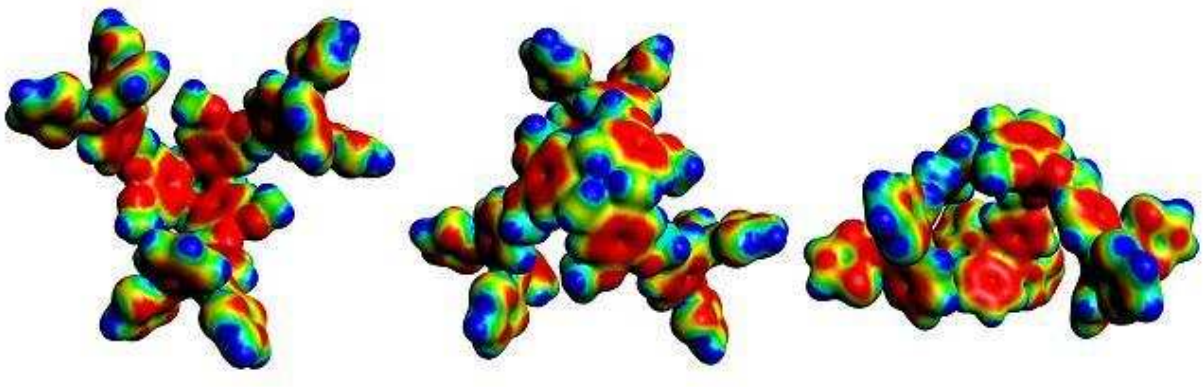

Figure S 23*:* Mapping of the electrostatic potential onto an electron density isosurface of empty receptor (BP86/DZP). From left to right: inner, outer and side views**.**

In the complexes (Figure S 24), the electrostatic potential for fullerenes is no longer as positive as in the case of free fullerenes, which suggest that either charge transfer or strong polarization occurred upon complexation.

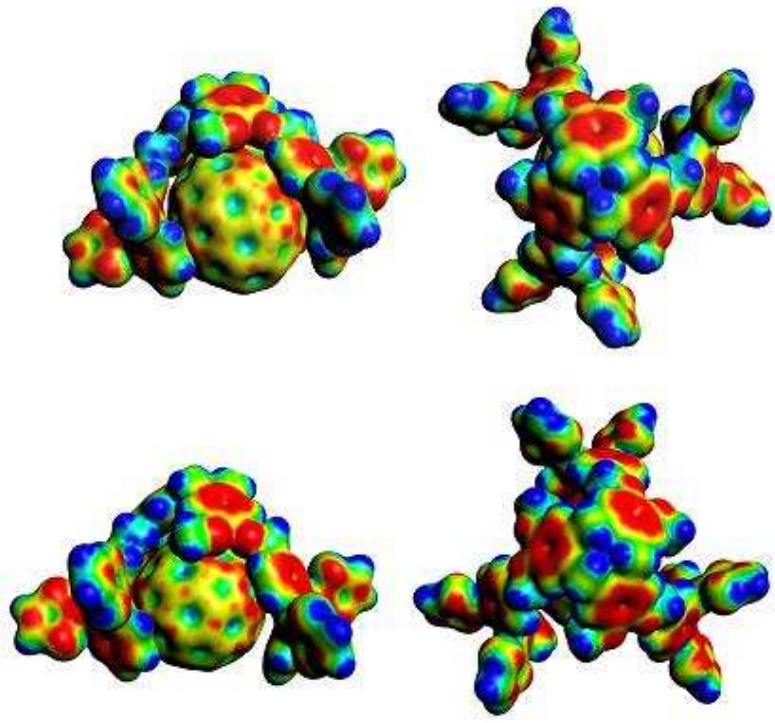

Figure S 24: Mapping of the electrostatic potential onto an electron density isosurface of the complexes (BP86/DZP) C_{70}**@exTTF-CTV** (top) and C_{60}**@exTTF-CTV** (bottom) in the ground state.

Indeed, analysis of the Mulliken atomic charges indicates clearly that the receptor and the fullerene moieties in the complex are slightly positively and negatively charged, respectively (see

Table 1**Error! Reference source not found.**, charge analysis), so charge transfer from the host to the guest. Note that the value is larger for C_{70} (0.31) than for C_{60} (0.25).

Table 1: Total Energies for the host (H), the guest (G) and the complex (HG) at the geometry of the complex, and of the host free (H_f) at the BP86/TZP and at the BH&H/TZ2P levels. Energies of the HOMO, the LUMO, and Mulliken charges (BP86/TZP).

C_{60}@exTTF-CTV Complex						
	BP86/TZP	**BH&H/TZ2P**	**HOMO**	**LUMO**	**Mulliken Charges**	
	E (kcal·mol^{-1})	**E (kcal·mol^{-1})**	**E (eV)**	**E (eV)**	**Q H-HG**	**q G-HG**
Host (H)	-24414.58	-36530.48	-4.166	-2.059		
Guest (G)	-11966.41	-17793.22	-6.238	-4.586		
Complex (HG)	-36369.38	-54347.38	-4.191	-3.646	0.25	-0.25
Host Free (Hf)	-24422.26	-36539.11				
Deformation Host	7.7	8.6				
Binding Energy	+19.3	-15.0				
C_{70}@exTTF-CTV Complex						
	BP86/TZP	**BH&H/TZ2P**	**HOMO**	**LUMO**	**Mulliken Charges**	
	E (kcal·mol^{-1})	**E (kcal·mol^{-1})**	**E (eV)**	**E (eV)**	**Q H-HG**	**q G-HG**
Host (H)	-24419.82	-36537.62	-4.104	-2.103		
Guest (G)	-14022.76	-20823.16	-6.252	-4.543		
Complex (HG)	-38426.79	-57384.40	-4.145	-3.567	0.31	-0.31
Host Free (Hf)	-24422.26	-36539.11				
Deformation Host	2.4	1.5				
Binding Energy	+18.2	-22.1				

As it can be seen in Table 1, the energy of the HOMO of the complex resembles the HOMO is located in the exTTF fragments, while the LUMO is located in the fullerene molecule. Besides, in both complexes the HOMO-LUMO gap is not very large, which facilitates the charge transfer from the receptor to the fullerene.

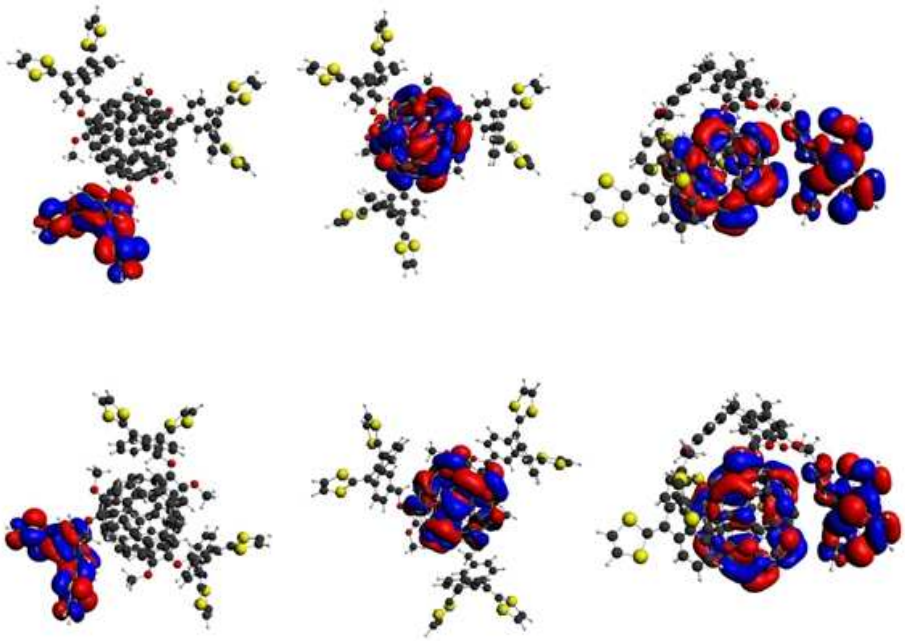

Figure S 25: Representation of different views of the HOMO, the LUMO, and both orbitals (electron density contours 0.015 e bohr^{-3}) in the complexes. Top: C_{60}@**exTTF-CTV** complex; Bottom: C_{70}@**exTTF-CTV** complex.

UV-Vis excitation energies were determined at the BP86/DZP level by means of the time-dependent DFT (TDDFT) approach. A total number of 300 singlet-singlet excitations were included.

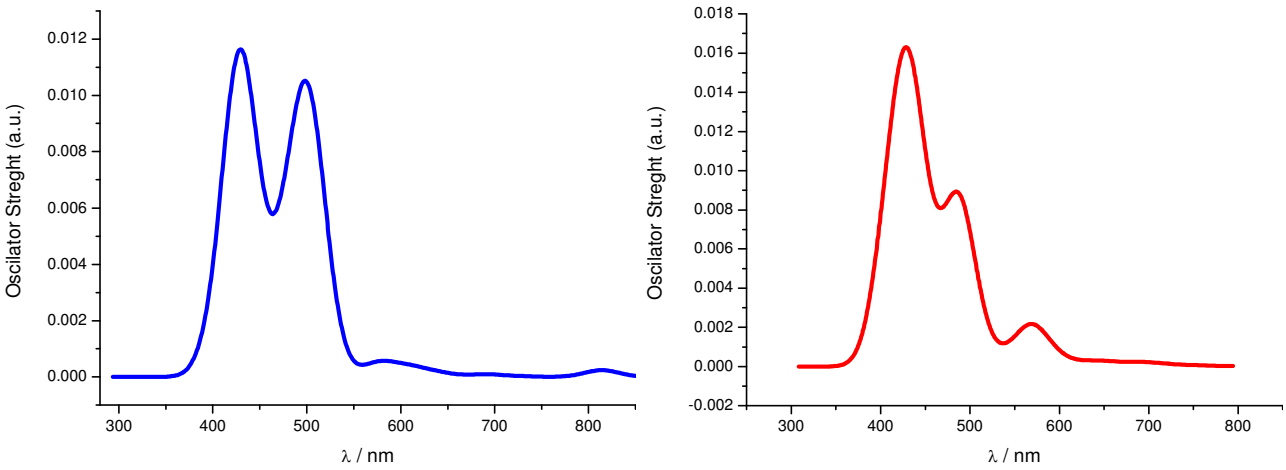

Figure S 26: Simulated UV spectrum of C_{60}@**exTTF-CTV** (left) and C_{70}@**exTTF-CTV** (right) complexes.